

Localized Phase Structures Growing Out of Quantum Fluctuations in a Quench of Tunnel-coupled Atomic Condensates

Clemens Neuenhahn,^{1,*} Anatoli Polkovnikov,² and Florian Marquardt¹

¹*Friedrich-Alexander-Universität Erlangen-Nürnberg, Institute for Theoretical Physics II, Staudtstraße 7, 91058 Erlangen, Germany*

²*Department of Physics, Boston University, 590 Commonwealth Avenue, Boston, Massachusetts 02215, USA*
(Received 8 February 2012; published 21 August 2012)

We investigate the relative phase between two weakly interacting 1D condensates of bosonic atoms after suddenly switching on the tunnel coupling. The following phase dynamics is governed by the quantum sine-Gordon equation. In the semiclassical limit of weak interactions, we observe the parametric amplification of quantum fluctuations leading to the formation of breathers with a finite lifetime. The typical lifetime and density of these “quasibreathers” are derived employing exact solutions of the classical sine-Gordon equation. Both depend on the initial relative phase between the condensates, which is considered as a tunable parameter.

DOI: 10.1103/PhysRevLett.109.085304

PACS numbers: 67.85.De, 03.75.Kk, 03.75.Lm, 05.30.Jp

Dynamical instabilities can amplify spatial field fluctuations drastically. If the instability provides sufficient energy, even quantum zero-point fluctuations can trigger the formation of macroscopic field patterns. For instance, in some cosmological scenarios of the inflationary stage of the universe, following a slow-roll, a scalar inflaton field performs oscillations around the minimum of the corresponding inflaton potential. Thereby, resonant spatial fluctuations are amplified parametrically. For a rather generic class of potentials these can end in long-lived, local concentrations of energy, so-called “oscillons” (e.g., Refs. [1–4]).

In this work, we argue that analogous nonequilibrium phenomena should be observable in experiments with a pair of weakly interacting quasi-1D clouds of cold, bosonic atoms [5,6]. After suddenly turning on the tunnel coupling between the condensates, the dynamics of the relative phase field $\hat{\phi}$ is governed by the integrable quantum sine-Gordon model [7]

$$\frac{d^2 \hat{\phi}}{dt^2} - \frac{d^2 \hat{\phi}}{dx^2} + \frac{m^2}{\beta} \sin \beta \hat{\phi} = 0, \quad (1)$$

where the “mass” m depends on the tunnel amplitude, such that $m(t) = m\Theta(t)$ for this quench. The phase has been rescaled, and for weak interactions $\beta \ll 1$.

The sine-Gordon model (SGM) is one of the most prominent prototypical models of low-dimensional condensed-matter systems. Currently, quenches in the SGM are under intense investigation (e.g., Refs. [8–13]).

Here, we propose that the spatially averaged value Φ of the relative phase field is tuned to some value Φ_0 right before the quench [e.g., this might be achieved by slightly tilting the transversal double-well potential confining the BECs, cf. Fig. 1(a)]. The subsequent phase dynamics can be directly observed in matter wave interference experiments [5,6].

At short times, Φ will perform Josephson oscillations [Fig. 1(b)] according to $d^2 \Phi / dt^2 = -\beta^{-1} m^2 \sin \beta \Phi$. However, these are linearly unstable [14,15] in the presence of inhomogeneous quantum fluctuations which are parametrically amplified at certain wavelengths [Fig. 1(c)]. As we will show in this paper, due to this instability at some later point the dynamics becomes fully nonlinear and one observes the formation of sharply localized and oscillating patterns in the phase-field [Fig. 1(c)]. It will be shown below that they can be related to particular exact

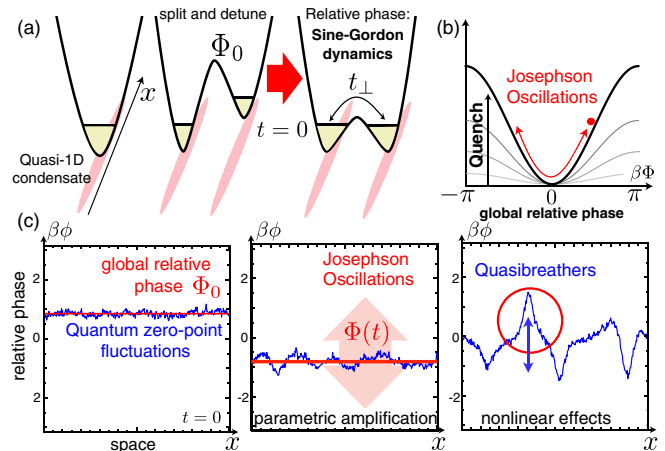


FIG. 1 (color online). (a) Proposed experimental protocol. A single quasi-1D condensate is split and the global phase is tuned to Φ_0 . Switching on the tunnel-coupling, the dynamics of the relative phase obeys the quantum sine-Gordon equation. (b) At short times, the global phase performs Josephson oscillations. (c) Single run of TWA (see main text) with $\beta\Phi_0 = 0.25\pi$. Spatial quantum fluctuations are amplified parametrically. Eventually, the nonlinearity of the sine-Gordon equation kicks in and quasibreathers (breathers with a finite lifetime) form. The big (thin), vertical arrow indicates the Josephson (quasibreather) oscillations.

solutions of the classical SGM obtained from the Bäcklund transformation (following Ref. [16]). These quasibreathers (QBs) have a finite lifetime (in contrast to the well-known breather solutions), and we find good evidence that a quasiequilibrium steady state with a finite density of such excitations develops at long times.

A similar pattern formation in an elongated condensate seeded by quantum fluctuations was observed experimentally [17]. After switching the positive scattering length to small negative values, trains of bright solitons emerged. It was argued [18] that these trains can be traced back to phonon excitations becoming unstable after the interaction quench; i.e., their frequencies become imaginary. Another interesting example is [12] predicting the formation of “supersolitons” after a combined mass-interaction quench in the SGM to the so-called Luther-Emery point ($\beta^2 = 4\pi$). At this special point, the system can be mapped to free fermions [representing noninteracting (anti)solitons of the classical SGM].

In contrast, the amplification observed in the present case crucially relies on nonlinearities. For the considered quench, due to the intrinsic instability, a simple approximation of the SGM in terms of noninteracting, massive phonons is invalid, even though $\beta \ll 1$. Instead, we employ the truncated Wigner-approximation (e.g., Ref. [19]) (TWA). The basic idea behind TWA is to simulate classical field equations, but with quantum-mechanical fluctuations as stochastic initial conditions. In the limit of $\beta \rightarrow 0$, TWA is expected to become reliable as it can be shown that β plays the role of an effective Planck’s constant [19]. It describes correctly the linear dynamics during the parametric amplification. Once QBs form, occupation numbers are already large (of the order $\sim 1/\beta^2$) such that a semiclassical description (provided by TWA) should continue to remain valid. The great advantage of TWA is that it serves snapshots [Fig. 1(c)] of the phase field $\phi(x, t)$ run-by-run, which can be compared directly to the experimental observations.

In the following, we introduce the model and demonstrate that the proposed setup should be well within the reach of present experiments. After a discussion of the numerical findings obtained from TWA, we will introduce the analytical quasibreather solutions of the classical SGM. We demonstrate that these solutions are well suited to explain the main physical features as predicted by TWA. Eventually, we argue that a statistical analysis of $\phi(x, t)$, experimentally obtained at a single time t per run, could reveal the distinctive signature of QBs.

Model.—It was argued [7] that on scales larger than the condensate healing length ξ_h , the dynamics of the relative phase between condensates $\hat{\phi} \equiv (\hat{\phi}_1 - \hat{\phi}_2)/\sqrt{2}$ (and of the density field $\hat{\Pi}$, fulfilling $[\hat{\Pi}(x), \hat{\phi}(x')] = i\delta(x - x')$) is governed by the quantum SGM. After rescaling the fields ($\hat{\phi} \mapsto \sqrt{\pi/K}\hat{\phi}$ and $\hat{\Pi} \mapsto \sqrt{K/\pi}\hat{\Pi}$), the Hamiltonian reads

$$\hat{H} = \frac{\hbar v_s}{2} \int dx [\hat{\Pi}^2 + (\partial_x \hat{\phi})^2] - \frac{m^2}{\beta^2} \int dx \cos \beta \hat{\phi}. \quad (2)$$

The repulsive short-range interaction, characterized by the Luttinger parameter $K \in [1, \infty]$, enters $\beta = \sqrt{2\pi/K}$. For small interactions ($K \rightarrow \infty$), K is connected to the interaction parameter $\gamma = m_B g / \hbar^2 \rho_0$ via $K = \pi / \sqrt{\gamma}$ [20] (where g is the interaction strength, m_B the mass of the bosons and ρ_0 the mean density). Furthermore, there are the sound velocity $v_s = v_F / K$ (with $v_F = \hbar \pi \rho_0 / m_B$), and the effective mass $m = \sqrt{2t_\perp \rho_0} \beta$, where the tunnel-amplitude t_\perp between the condensates enters. The relevant length scale in the SGM, determining the width of breathers and solitons, is set by $\delta x = \sqrt{\hbar v_s / m}$. The Josephson frequency is $\omega_J = m \sqrt{v_s / \hbar}$. In the following, we set $v_s = \hbar = 1$.

The sine-Gordon model should be a sound description for $\xi_h / \delta x \ll 1$ ($\xi_h \sim 1 / \rho_0 \sqrt{\gamma}$). In this limit, we expect that a residual (integrability breaking) coupling to the symmetric phase mode [21,22] does not qualitatively alter the dynamics of $\hat{\phi}$ on experimentally relevant time-scales (this is supported also by recent experiments [23]). Furthermore, (in contrast to Refs. [21,22], where $m = 0$ during the evolution) decoherence of the massive excitations in $\hat{\phi}$ due to the gapless excitations in the symmetric field is strongly suppressed due to energy and momentum conservation.

Experimental realizability.—The condition $\delta x \gg \xi_h$ translates into a lower bound for β : $\beta^2 \gg 4\rho_0^{-1} \sqrt{t_\perp m_B} / \hbar$. Within the present experimental setups, the condensate density can be widely tuned, e.g., in Ref. [24] the 1D density of Rb⁸⁷ atoms ranges from $\rho_0 = [\mathcal{O}(10^1) - \mathcal{O}(10^2)] \mu\text{m}^{-1}$. For a transverse trap frequency $\omega_\perp = 2\pi \times 4 \text{ kHz}$, with $g = 2\hbar\omega_\perp a_s$ and $a_s = 5.23 \times 10^{-9} \text{ m}$, one can realize K up to ~ 50 ; i.e., small values of the sine-Gordon parameter $\beta = \mathcal{O}(10^{-1})$ are well achievable. Eventually, the tunnel amplitude can be tuned up to $t_\perp / (2\pi \times \hbar) = \mathcal{O}(10^2) \text{ Hz}$ [5]. For large densities $\rho_0 = 100 \mu\text{m}^{-1}$ the lower bound on β is $\mathcal{O}(10^{-1})$, as well. In all numerical simulations, we use $\beta = 0.1$. We conclude that after some fine-tuning of the experimental parameters, the proposed setup should be within reach.

Numerical results.—Before the quench, the phase field ϕ is given by the offset Φ_0 plus the small zero-point fluctuations of the free theory [Eq. (2) with $m = 0$]. Within TWA, the fluctuations of the ϕ and Π modes are initialized according to their Gaussian Wigner distribution [19], omitting the $q = 0$ mode block. All numerical simulations are performed on a lattice. To avoid artifacts due to the discreteness of the numerical implementation, we chose the mass such that δx is of the order $\mathcal{O}(1)$ in terms of the lattice spacing.

This initial state should be experimentally achievable. One should start from the ground state at strong tunnel coupling (very large m), where the relative phase

$\phi(x) = 0$. During a slow linear ramp-down of the tunnel amplitude, all modes $\phi_{q \neq 0}$ will follow their time-dependent ground state. It can be shown that the global phase Φ at the end of this process obeys $\beta^2 \langle \Phi^2 \rangle \sim 1/\xi_h \rho_0$, which remains small as long as the number of bosons within the healing length is large. An additional potential tilt will produce a fixed phase offset $\Phi \simeq \Phi_0$. We will focus on rather small $0 < \beta\Phi_0 \leq 1$. For $\beta\Phi_0 \rightarrow \pi$, in addition to breathers one observes the formation of solitons. Finally, we note that this phase-tuning becomes impossible for infinite systems. This is due to the logarithmic divergence of phase fluctuations with system size L in the massless ground state, i.e., $\beta^2 \langle \delta\hat{\phi}^2 \rangle \sim \beta^2 \ln L$. However, these are largely suppressed in the semiclassical limit $\beta \ll 1$. We always choose the system size such that the initial overall relative phase is well defined.

In Fig. 2, the phase field for a single run of TWA is shown. At small times, the field is dominated by $\Phi(t)$ performing ordinary Josephson oscillations. At this point, the inhomogeneous part $\delta\phi(x, t)$ of $\phi = \Phi + \delta\phi$ can be treated as a small perturbation. The modes obey $\partial_t^2 \phi_k + (k^2 + m^2 \cos[\beta\Phi(t)])\phi_k \simeq 0$ for all $k \neq 0$; i.e., these are phonons with a periodically modulated mass. Modes with $|k| \in [0, m \sin|\beta\Phi_0/2|]$ are parametrically amplified yielding $\phi_k(t) \sim e^{\Gamma_k t}$. The amplification rates Γ_k for this linear regime (here displayed for $\beta\Phi_0 \leq 1$) [see Fig. 3(a)]

$$2\Gamma_k \simeq |k| \sqrt{\sin^2(\beta\Phi_0/2) - k^2/m^2}, \quad (3)$$

were found in Ref. [14], neglecting the damping of the driving Φ -mode. After some time, nonlinear interactions between the amplified modes become important and lead to the formation of sharply localized oscillating structures

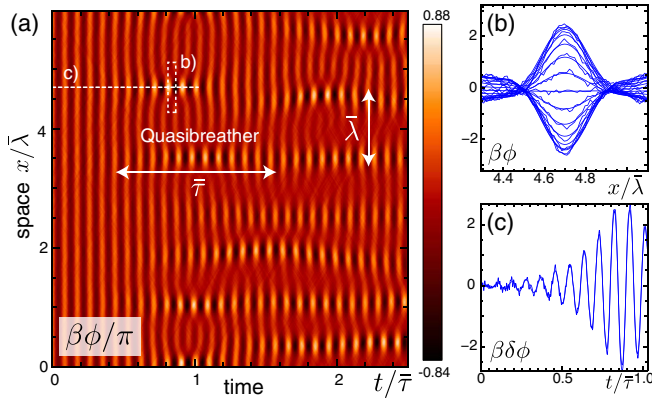


FIG. 2 (color online). (a) Space-time plot of the phase field for a single simulation run. (b) Spatial cut through the quasibreather highlighted in (a) over one breather period (thin blue line; thick blue line: filtering out irrelevant short wavelength fluctuations). (c) Temporal cut through the emerging QB taken at its center. $\delta\phi = \phi - \Phi$ is obtained by subtracting the spatially averaged field $\Phi = \frac{1}{L} \int_0^L dx \phi$. One observes the exponential amplification of initial quantum fluctuations. Here, $\beta\Phi_0 = 0.3\pi$.

(here denoted as quasibreathers), which constitute the main phenomenon discussed in our paper. Once these localized oscillations get out of phase with respect to the background oscillations of Φ , their energy is depleted again. One arrives at a steady-state, where QBs are randomly created and decay, with a typical lifetime $\bar{\tau}$ and a mean spatial distance $\bar{\lambda}$ (cf. Fig. 2). All these statistical quantities crucially depend on the initial value Φ_0 . It turns out that these localized modulations in the stochastic phase field can be connected to certain exact solutions of the SGM. These solutions, to be discussed in the following, are standing breathers riding on top of a homogeneous and oscillating background. We will demonstrate that this set of solutions is well suited to describe the numerical observations and provides analytical insight into the dependence of $\bar{\lambda}$ and $\bar{\tau}$ on Φ_0 .

Quasibreathers.—A Bäcklund transformation (see, for instance, Ref. [16]) allows us to “add” (anti)solitons to a given solution of the SGM, here taken to be the spatially

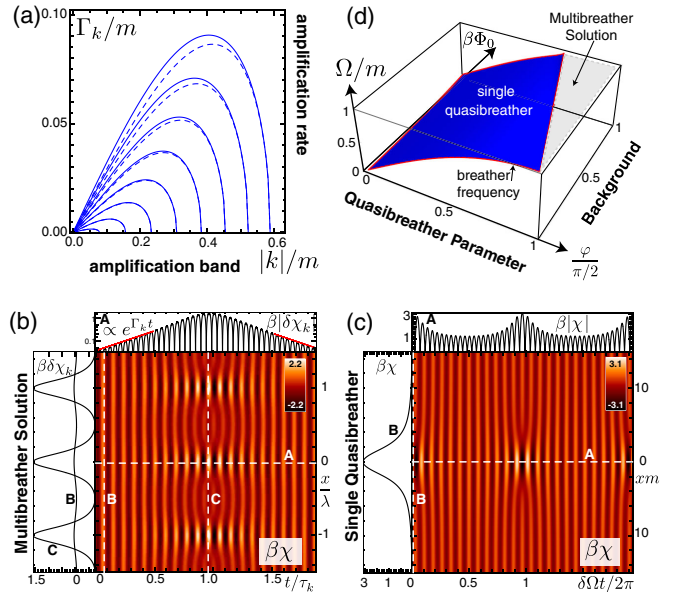


FIG. 3 (color online). (a) Phononic zero-point fluctuations are amplified parametrically driven by the overall phase Φ performing Josephson oscillations. Corresponding amplification rate Γ_k of phonons with wave number k for $\beta\Phi_0/\pi \in 0.05-0.4$ according to Eq. (3) (dashed line). Solid lines show the rate obtained from the “multibreather” solution Eq. (5). (b) Plot of a (spatially periodic) multibreather solution reducing to a driven phonon with wave number $k = m\beta\Phi_0/\sqrt{8}$ for $t/\tau_k \rightarrow -\infty$. Cut A shows the parametric amplification of this phonon (B) driven by the oscillating background (we plot $\delta\chi_k$, subtracting this background). It provides “seeds” for the formation of quasibreathers (C) with a lifetime τ_k . Here, $\beta\Phi_0 = 0.3\pi$. (c) Plot of a single quasibreather (periodic in time) with $\beta\Phi_0 = 0.3\pi$ and $\varphi = 1.02$. (d) Mean frequency $\Omega \equiv m - \delta\Omega$ of a single quasibreather ($|\sin\varphi| < |\cos\frac{\beta\Phi_0}{2}|$) depending on the amplitude of the background oscillations and the parameter φ . For $\Phi_0 = 0$, one restores the unperturbed breather frequency $\Omega = m \sin\varphi$.

homogeneous solution $\Phi(t)$ with $\Phi(0) = \Phi_0$ and $\dot{\Phi}(0) = 0$. Adapting the approach of Ref. [16], we obtain quasibreather solutions by adding a (standing) soliton and the corresponding antisoliton to Φ . A standing SGM-breather is characterized by its amplitude (e.g., Ref. [25]). The solutions here depend in addition on the amplitude of the underlying background oscillations Φ_0 (furthermore, there is a minor dependence on the precise value of the relative phase Δ_0 between breather and background at $t = 0$). They have the form

$$\chi(x, t) = \frac{4}{\beta} \arctan[\mathcal{G}(x, t; \Phi_0, \Delta_0, \varphi)] + \Phi(t). \quad (4)$$

For $\Phi_0 = 0$, the parameter $\varphi \in [0, \pi/2]$ determines the unperturbed breather frequency $m \sin \varphi$ and $\max \chi = \beta^{-1}(2\pi - 4\varphi)$. An explicit expression for \mathcal{G} and a discussion of Eq. (4) are given in Ref. [26]. Here, we focus on the most relevant features in the limit $\beta\Phi_0 \lesssim 1$.

The central observation is that by placing a breather on top of the oscillating background, its amplitude becomes time-dependent [see Figs. 3(b) and 3(c)]. The background $\Phi(t)$ amplifies the breather while the frequency of the latter decreases. This is due to the fact that the effective curvature of the cosine potential decreases for larger field amplitudes. Eventually, both run out of phase and, subsequently, the breather gets damped. The relative phase drift occurs at a frequency

$$\delta\Omega(\varphi, \Phi_0) = \frac{m\sqrt{|\cos^2(\beta\Phi_0/2) - \sin^2\varphi|} \cos\varphi}{1 + \sin\varphi}. \quad (5)$$

As long as $\sin\varphi < \cos(\beta\Phi_0/2)$, χ describes a single breather whose amplitude is modulated with a period $2\pi/\delta\Omega$ [Fig. 3(c)]. This constitutes a stable QB solution of the SGM. As the background oscillates at frequency m , one can understand $\Omega \equiv m - \delta\Omega$ as the mean frequency of the quasibreather [Fig. 3(d)].

For $\sin\varphi \rightarrow \cos(\beta\Phi_0/2)$, however, the period diverges. In fact, it turns out that for $\sin\varphi > \cos(\beta\Phi_0/2)$, χ is periodic in space rather than in time [Fig. 3(b)]. It describes a set of quasibreaters at distance $2\pi/k = 2\pi m^{-1}|\cos^2(\beta\Phi_0/2) - \sin^2\varphi|^{-1/2}$.

These multibreather solutions have remarkable properties. For $t \rightarrow -\infty$, they reduce to a phonon $\delta\chi_k$ with wave number k , superimposed on the oscillating background. It is amplified parametrically, yielding

$$\delta\chi_k \propto e^{\Gamma_k t} \zeta(t) \cos kx, \quad (6)$$

where $\zeta(t)$ is a periodic function and the amplification rate $\Gamma_k \equiv \delta\Omega(\varphi(k), \Phi_0)$. This rate is in agreement with the results in Eq. (3) for small $\beta\Phi_0$. At later times, the characteristic breather peaks form [Fig. 3(b)], exist during a time set by $\tau_k = 4/\Gamma_k$, and decay again for $t \rightarrow \infty$. Note that χ , therefore, describes the prototypical formation of QBs out of fluctuations in a single mode ϕ_k .

Our numerical analysis shows (see below) that one can infer the properties of typical QBs observed within the stochastic TWA from these ideal multibreather solutions χ . In a given run, zero-point fluctuations in all modes are present. However, in the weakly interacting limit ($\beta \ll 1$), the parametric instability automatically filters out modes with $k \approx \bar{k}$, where $\bar{k} \simeq m\beta\Phi_0/\sqrt{8}$ denotes the maximally amplified mode. Thus, the typical distance between QBs is roughly given by $\bar{\lambda} = 2\pi/\bar{k}$. Although the strictly periodic multibreather solution χ is not directly observed, individual QBs are well described by χ as long as their amplitude is large enough compared to the noisy background. Typical QBs decay after a lifetime $\bar{\tau} \equiv \tau_{\bar{k}}$ [cf. Fig. 3(b)]. When their amplitude is depleted down to the noise level, the exact solution ceases to be relevant. Then the background oscillations initiate the amplification process again, leading to the formation of new QBs. This explains the observed stochastic creation and annihilation of QBs at large times $\Gamma_{\bar{k}} t \gg 1$.

Statistical analysis.—These predictions agree well with the statistical analysis of the quench within TWA. For every run, we numerically track all QBs, showing their shape $\phi_{\text{QB}}(x)$ at the time of maximum amplitude [Fig. 4(a)]. A comparison of the mean QB shape $\langle \phi_{\text{QB}} \rangle$ and χ (with $k = \bar{k}$) shows excellent agreement. Note that no fit parameter enters here.

Finally, Fig. 4(b) shows the equal-time correlation function $C_{\phi\phi}(x, t) = \langle \hat{\phi}(x, t)\hat{\phi}(0, t) \rangle - \langle \hat{\phi}(0, t) \rangle^2$ evaluated with TWA. For $t/\bar{\tau} > 1$, it saturates, indicating that the field enters a statistical steady state. One can find a decent approximation [26] for $C_{\phi\phi}$ at large times $t \gg \bar{\tau}$, assuming that $\phi(x, t)$ can be represented as a sum of

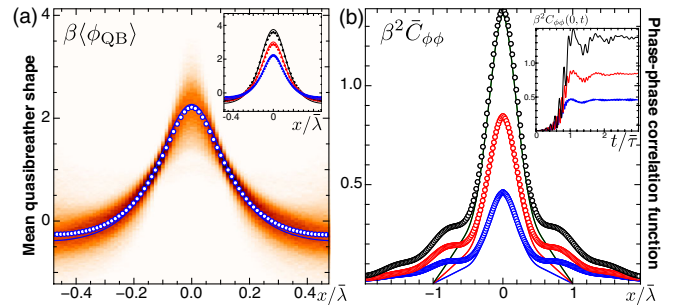


FIG. 4 (color online). (a) Mean shape of QBs taken at their maximal value, obtained from TWA (blue dots) and full distribution of shapes (color plot). We track QBs numerically run-by-run in the interval $t/\bar{\tau} \in [0.5, 4]$ for $\beta\Phi_0/\pi = 0.3$. Comparison to the analytical “multibreather” solution $\chi(x, 0)$ with \bar{k} (blue, solid line; $\Delta_0 = 0$) shows almost perfect agreement. Inset) Various $\beta\Phi_0/\pi = 0.3, 0.4, 0.5$ (from bottom to top). No fit parameter enters. (b) Correlation function $C_{\phi\phi}$, averaged over time $t/\bar{\tau} \in [2.25, 3]$ (dots) with $\beta\Phi_0/\pi = 0.3, 0.4, 0.5$ (from bottom to top). Locally, it agrees well with Eq. (7). Inset shows $C_{\phi\phi}(0, t)$, demonstrating that the field enters a steady state for $\beta\Phi_0/\pi = 0.3, 0.4, 0.5$, from bottom to top.

independent QBs, at an average density $1/\bar{\lambda}\bar{\tau}$ in the (x, t) -plane:

$$C_{\phi\phi} \approx \int_{-\bar{\lambda}/2}^{\bar{\lambda}/2} \frac{dx_0}{\bar{\lambda}} \int_{-\bar{\tau}/2}^{\bar{\tau}/2} \frac{dt_0}{\bar{\tau}} \tilde{\chi}(x; x_0, t_0) \tilde{\chi}(0; x_0, t_0), \quad (7)$$

which describes the core part of $C_{\phi\phi}$ fairly well (cf. Fig. 4). Here, a single QB from the multibreather solution centered at x_0 enters: $\tilde{\chi}(x; x_0, t_0) = \Theta(\frac{\bar{\lambda}}{2} - |x - x_0|) \chi(x - x_0, t_0; \bar{k})$ (Θ denotes the heavy-side step function).

This correlation function is directly accessible in experiments and should distinctively reveal the presence of QBs. Moreover, one could simply perform a direct statistical analysis of ϕ [cf. Fig. 4(a)].

Summary.—We predict the formation of localized modulations in the relative phase field, after suddenly switching on the tunnel coupling between a pair of quasi-1D condensates. These quasibreathers grow out of initial quantum fluctuations, mimicking processes that are crucially important in other areas like cosmology. They can be well described by exact analytical solutions of the sine-Gordon model. We derived their mean lifetime and density after the system reaches a statistical steady state. These predictions are consistent with our numerical simulations. An experimental realization, even with present setups, seems to be within reach.

We thank J. Schmiedmayer for fruitful discussions. Financial support by the Emmy-Noether program and the SFB/TR 12 is gratefully acknowledged. C.N. thanks A.P. for his hospitality at BU.

*clemens.neuenhahn@physik.uni-erlangen.de

- [1] M. Gleiser and R. C. Howell, *Phys. Rev. E* **68**, 065203 (2003).
- [2] M. A. Amin, R. Easter, and H. Finkel, *J. Cosmol. Astropart. Phys.* **12** (2010) 001.
- [3] E. Farhi, N. Graham, A. H. Guth, N. Iqbal, R. R. Rosales, and N. Stamatopoulos, *Phys. Rev. D* **77**, 085019 (2008).
- [4] M. A. Amin, R. Easter, H. Finkel, R. Flauger, and M. P. Hertzberg, *Phys. Rev. Lett.* **108**, 241302 (2012).
- [5] S. Hofferberth, I. Lesanovsky, B. Fischer, T. Schumm, and J. Schmiedmayer, *Nature (London)* **449**, 324 (2007).
- [6] T. Betz, S. Manz, R. Bücke, T. Berrada, C. Koller, G. Kazakov, I. E. Mazets, H.-P. Stimming, A. Perrin, T. Schumm, and J. Schmiedmayer, *Phys. Rev. Lett.* **106**, 020407 (2011).
- [7] V. Gritsev, A. Polkovnikov, and E. Demler, *Phys. Rev. B* **75**, 174511 (2007).
- [8] V. Gritsev, E. Demler, M. Lukin, and A. Polkovnikov, *Phys. Rev. Lett.* **99**, 200404 (2007).
- [9] C. D. Grandi, R. A. Barankov, and A. Polkovnikov, *Phys. Rev. Lett.* **101**, 230402 (2008).
- [10] J. Lancaster, E. Gull, and A. Mitra, *Phys. Rev. B* **82**, 235124 (2010).
- [11] A. Iucci and M. A. Cazalilla, *New J. Phys.* **12**, 055019 (2010).
- [12] M. S. Foster, E. A. Yuzbashyan, and B. L. Altshuler, *Phys. Rev. Lett.* **105**, 135701 (2010).
- [13] J. Sabio and S. Kehrein, *New J. Phys.* **12**, 055008 (2010).
- [14] P. B. Greene, L. Kofman, and A. A. Starobinsky, *Nucl. Phys.* **B543**, 423 (1999).
- [15] I. Bouchoule, *Eur. Phys. J. D* **35**, 147 (2005).
- [16] D. W. McLaughlin and A. C. Scott, *Phys. Rev. A* **18**, 1652 (1978).
- [17] K. E. Strecker, G. B. Partridge, A. G. Truscott, and R. G. Hulet, *Nature (London)* **417**, 150 (2002).
- [18] U. A. Khawaja, H. T. C. Stoof, R. G. Hulet, K. E. Strecker, and G. B. Partridge, *Phys. Rev. Lett.* **89**, 200404 (2002).
- [19] A. Polkovnikov, *Ann. Phys. (N.Y.)* **325**, 1790 (2010).
- [20] M. A. Cazalilla, *J. Phys. B* **37**, S1 (2004).
- [21] A. A. Burkov, M. D. Lukin, and E. Demler, *Phys. Rev. Lett.* **98**, 200404 (2007).
- [22] I. E. Mazets and J. Schmiedmayer, *Eur. Phys. J. B* **68**, 335 (2009).
- [23] M. Gring, M. Kuhnert, T. Langen, T. Kitagawa, B. Rauer, M. Schreitl, I. Mazets, D. A. Smith, E. Demler, and J. Schmiedmayer, [arXiv:1112.0013v1](https://arxiv.org/abs/1112.0013v1).
- [24] P. Krüger, S. Hofferberth, I. E. Mazets, I. Lesanovsky, and J. Schmiedmayer, *Phys. Rev. Lett.* **105**, 265302 (2010).
- [25] K. Maki and H. Takayama, *Phys. Rev. B* **20**, 5002 (1979).
- [26] See Supplemental Material at <http://link.aps.org/supplemental/10.1103/PhysRevLett.109.085304> for details.